ISSN 0097-8078, Water Resources, 2017, Vol. 44, No. 6, pp. 808–819. © Pleiades Publishing, Ltd., 2017.
Original Russian Text © E.N. Dolgopolova, 2017, published in Vodnye Resursy, 2017, Vol. 44, No. 6, pp. 628–640.

HYDROPHYSICAL PROCESSES

Tidal Waves at Mezen Mouth and Surge-Wave Formation Conditions

E. N. Dolgopolova

Water Problems Institute, Russian Academy of Sciences, Moscow, 119333 Russia
e-mail: dolgopolova@gmail.com

Received October 22, 2015; in final form, May 30, 2016

Abstract—The factors that govern the distribution and transformation of tidal waves in the macrotidal estuary of the Mezen River have been considered, including tide range in the mouth section, water discharge in the river's lower reaches, estuary shape, and bed resistance coefficient. Data on variations of water discharge over period 1920–2008 are given. The parameters of estuary channel narrowing in horizontal and vertical sections have been considered. The effect of narrowing and bed hydraulic friction on tide wave amplitude has been evaluated. Froude number values for the tidal estuary suggest that tidal bore can form at the Mezen mouth. The conditions of the propagation of tidal waves to the mouths of different rivers and tidal bore formation in them are considered.

Keywords: river mouth, tide, tidal wave transformation, estuary shape, tidal bore

DOI: 10.1134/S0097807817060033

INTRODUCTION

The results of first studies of the hydrological regime of Mezen mouth were published in 1932, and active studies in this region were carried out in 1958–1988 as a component of the beginning works for designing a tidal power plant in Mezen Gulf. Exhaustive information about studies at Mezen mouth is given in [2]. The studies in [2] provided material used by the authors of [17] to identify the effect of tide-induced water level rise in the estuary, which was later described theoretically [7, 11]. The data obtained in the studies of the hydrological characteristics of the Mezen estuary, available at the time, were generalized in [13]. The authors of [13, 17] identified transformations of the tidal wave in Mezen estuary. The characteristics of wave shape transformation along the estuary, i.e., the moments of water level rise and drop, are discussed, and plots of level variations at different points of the estuary during the spring and neap tides are given in [2, 3]. Notwithstanding the numerous studies of the Mezen estuary, none of the publications considers the possibility of tidal bore formation at the Mezen mouth and discusses the conditions required for its formation.

Tidal wave transformation during its propagation at the mouth depends to the greatest extent on the tide range in the mouth section, river water discharge, and the parameters of channel narrowing. It is assumed that at tide range $h > 4$ m, a tidal bore can form at a funnel-formed mouth, its formation probability increasing at low river water discharge [5, 22]. Therefore, to assess tidal wave transformation during its penetration into a river mouth one needs to have data on tides in the mouth section, river runoff variations, and channel narrowing parameters. In this case, the decrease in the cross-section area with decreasing channel width and depth may contribute differently to the possibility of tidal bore formation. The problem of the possibility of back-wave formation in a tidal estuary and the criterion of wave collapse is of great scientific and practical importance, as such waves have a considerable effect on the structure of currents at the mouth, sediment transport in the estuary, and the formation of the channel as a whole.

The large range of tides at the Mezen mouth (up to $h = 9.8$ m with a maximum during spring tide) [2] suggests that a tidal bore can form in this estuary. The results of studies of tidal wave transformations at the Mezen mouth given in [2] along with data on flow velocities and estuary channel shape [16] were used to analyze the possibility of tidal bore formation at the Mezen mouth and suggested the conclusion that a tidal bore exists in this estuary [23]. Cases of tidal bore (or swell) formation at the Mezen mouth are mentioned in the literature [12, 33], and photo and video materials are available to support this conclusion. Figure 1 gives photographs of the first, highest, collapsing tidal bore (Fig. 1a) and several following waves (Fig. 1b) at the crossing Mezen T.–Kamenka V. [27]. In this paper, we consider the morphological–hydrological processes and the propagation of tidal waves in the Mezen estuary and analyze the formation conditions of a collapsing back wave in the estuary. The evolution of tidal wave shape and the conditions of tidal bore formation in the Mezen estuary are compared with those in other estuaries of the world. The role of

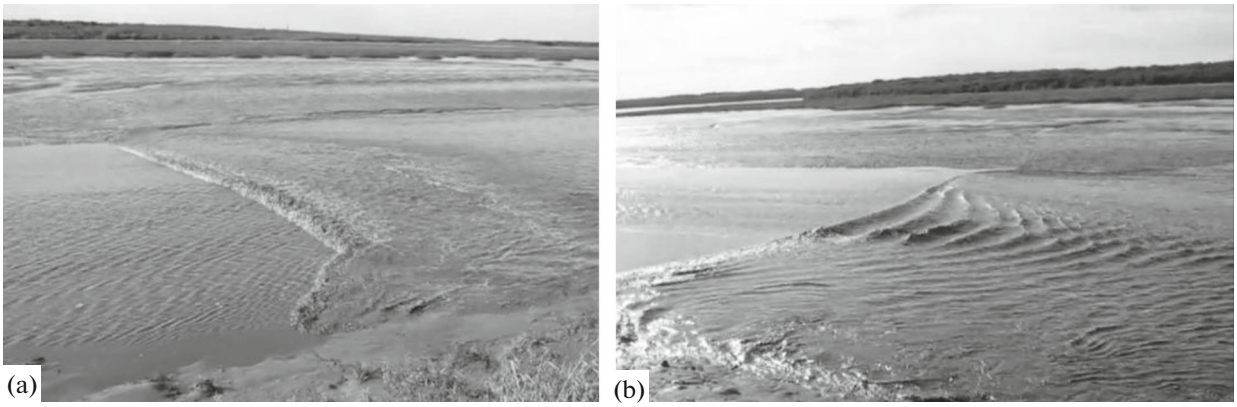

Fig. 1. Propagation of a tidal bore at the section of crossing between Mezen T. and Kamenka V.: the propagation of (a) the first, collapsing wave and (b) subsequent, smaller waves.

estuary depth in the evolution of tidal wave characteristics during its propagation along the estuary is examined.

TIDES AND WATER SALINITY AT THE ESTUARY OFFSHORE BOUNDARY (MEZEN GULF)

The physical processes in an estuary are governed by the interaction between the slightly saline and fresh waters in the estuary; this interaction depends on the marine and river factors. The tides and water salinity in the Mezen Gulf are the marine factors for the Mezen Estuary.

Dominating in the White Sea are regular semidiurnal tides [2, 9, 12]. The tidal wave from the Barents Sea propagates through the northern White Sea toward the northern boundary of the Mezen Gulf: Voronov Cape–Morzhovets Isl.–Konushin Cape. The formation of the tidal wave is governed by changes in the depths, which are 100–200 m in the central White Sea, decreasing to 20–30 m at the entry to the Mezen Gulf; the mean depth in the major portion of the gulf is 10 m. At the entry to the Mezen Gulf, the mean range of the spring tide h varies from 3.5 to 6.0 m, and that of the neap tide, from 2.2 to 4.6 m. From northwest to southeast, from Morzhovets Isl. to the Semzha R. mouth, h increases, on the average, from 7.6 m during spring tide to 5.3 m during neap tide with the maximal possible h during spring tide varying from 6.8 to 9.8 m [2]. Some transformation of tidal wave shape begins already in the shallow Mezen Gulf as can be seen from the decrease in the time of water level rise $t_1 = 5.15$ h compared with the time of its drop $t_2 = 7.15$ h at a distance of 16 km from the conventional line connecting Ryabinov Shape and Maslyanyi Shape [13].

Water salinity S on White Sea surface varies around 28–30‰ and drops to a minimum of 12‰ in the western Dvina Gulf [9, 13]. According to data in [2], in the spring, summer, and autumn, $S = 26$–28‰ on the surface in the Mezen Gulf at a distance of ~40 km from estuary mouth (EM).

MEZEN RIVER AND ITS MOUTH

The geographic position and the main characteristics of the Mezen R. are given in [15, 17, 18], and its mouth area is described in [2, 13, 17]. The river is 966 km long (Fig. 2a), its basin area is 78 000 km^2, the mean slope of the river being 0.38‰ [26]. The area of the Mezen Basin is composed of bedrocks: marl, clay, and sandstone, overlain by a bed of Quaternary deposits 15–20 m in thickness. The river originates on the Timan Ridge, the water divide of the Dvina–Pechora Basin, and empties into the Mezen Gulf, the White Sea, where it forms a macrotidal estuary. Downstream of the Vashka R. inflow, the banks of the river are bluff with a height of ~40 m, the right bank becoming higher and steeper with marl outcrops in precipices. The river channel becomes wider in this part, reaching 2.5 km at Mezen Town, and contains many islands, shallows, and rifts.

The river nourishment is mixed, including snow and rain. The spring flood takes place in May–June; summer and autumn rain freshets cause considerable short-time water level rises. Commonly, freezing begins in the upper reaches, gradually extending downstream. The river is under ice from late October to late April with the mean freeze-up period of 200 days [2, 3, 13]. An ice dam forms near Chetsa V. with no continuous ice sheet forming downstream of it [17]. This dam blocks river mouth reach, so the tide range at Kamenka V. decreases 3 times compared with the summer. The formation of an ice dam with a backwater effect in the estuary upstream of Chetsa V. causes a decrease in the tidal current velocity at Kamenka V. to 0.2 m/s.

The head of river mouth area (RMA) is defined by the maximal propagation of tidal water level variations in dry season; in the Mezen, it lies 90 km from the EM

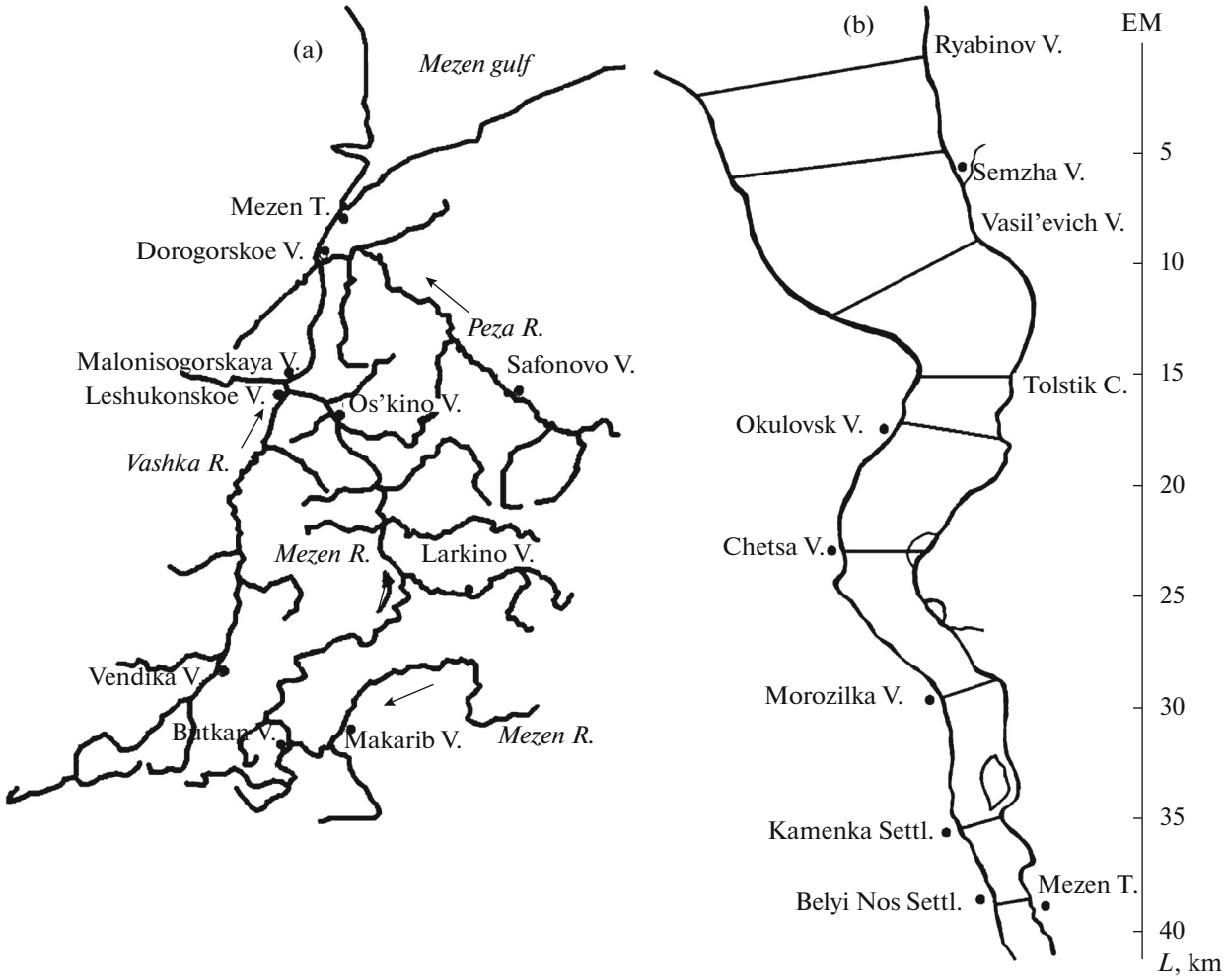

Fig. 2. (a) Schemes of the Mezen R. with its major tributaries and (b) its estuary with distances from EM to EH.

at the inflow of the large right-hand tributary, the Peza R., at Dorogorskoe V. (Fig. 2a) [13]. Strong tidal currents with velocities reaching 2.5 m/s cause rapid changes in estuary bed relief [17]. Near the estuary mouth section Ryabinov Cape–Maslyanyi Cape (Fig. 2b), the bed is covered by series of asymmetrical sand ridges (with lengths of up to 500 m and heights of ~1 m), moving toward the river. At a distance of 6 km from EM, sand-silt ridge rise above ebb tide level, forming vast drying shallows, separated by erosion channels. Two longitudinal low-tide sand ridges, 5–8 m in height, underlain by basic soil, outcropping on the bed of erosion channels, extend along the Semzha–Okulovsk reach. The ridges make the channel in this reach much narrower, as their width hear reaches 2.5 km. The tidal currents cause net flow of water and sediments toward estuary head in the western and eastern erosion channels. An ebb tide (direct) flow moves in the central channel between wattle shallows. In the reach Okulovsk–Mezen with narrowing channel, large side bars are attached to the right bank, some of them forming floodplain islands flood tide does not inundate. A chain of these islands extends along the right-hand bank of the estuary.

River Water Discharge in the Mezen Estuary

The Mezen is fed by many rivers and creeks, 20 of which empty into the river downstream of Malonisogorskaya V. [26], where a gauging station (g. s.) is located with the longest observation series of water discharges. The average annual water discharge Q at the Malonisogorskaya g. s. over 1921–2005 is 639 m^3/s (water runoff is 20.2 km^3/year), remaining nearly constant in the period under consideration (Fig. 3). Data on water discharges at Malonisogorskaya g. s. is basic, as no regular measurements of water discharge are carried out at the Mezen mouth. However, according to data in [2, 15], the average water discharge at the mouth is $Q = 868$ m^3/s (water runoff is 27.4 km^3/year), i.e., $Q = 229$ m^3/s is due to the tributaries downstream of Malonisogorskaya, which accounts for ~26.4% of water discharge at the mouth. This result can be used

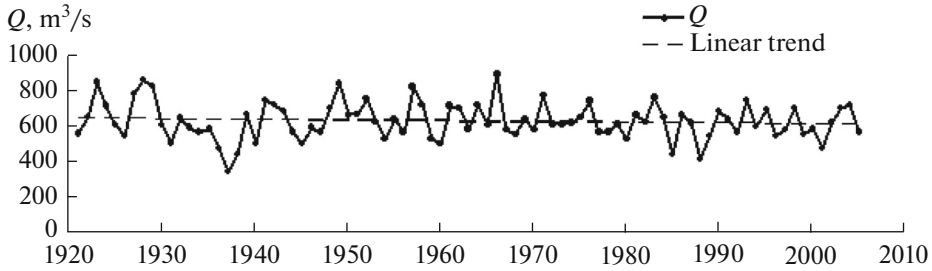

Fig. 3. Variation of mean water discharge Q at Malonisogorskaya g. s.

to evaluate the annual variations of water discharges at river mouth with the use of the hydrograph at Malonisogorskaya g. s., calculated from data [1] over period 1985–1987 at water flow close to normal annual (Fig. 4a). The comparison of the annual variations of Q at the Malonisogorskaya g. s. with the mean value Q over 1920–1976 at Mezen g. s. (Fig. 4b), according to data in [17], shows these values to be similar; therefore, the estimate of the annual variation of Q at Mezen mouth given above is justified. The summer low-flow period, when the formation of tidal bore in the estuary is most likely, falls into July and August with water discharges of 888 and 713 m^3/s, respectively.

RMA Zoning Taking into Account Hydrological Processes in the Estuary

Mezen Estuary has a classical funnel shape (Fig. 2b). The mouth section of the estuary lies abeam of Maslyanyi and Ryabinov capes. The estuary head (EH) of the Mezen R., determined by the maximal distance of saline water intrusion into the estuary, in accordance with [14], lies near Mezen Town at a distance $L = 40$ km from EM [13]. The maximal propagation distance of tidal level variations (96 km from EM [13]) determines the position of RMA head.

With the hydrological processes in the estuary taken into account, the length of the mouth offshore zone is determined by the position of 90% S isohaline of the sea, which corresponds to ~27‰ [14]. This isohaline lies 40 km from EM. In this case, the length of the mouth offshore zone is 40 km. With the northern boundary of the mouth offshore zone determined by morphological characteristics (1-m isobaths, passing along the line of Abramovskii Cape–Mgla R. mouth), the length of the offshore mouth zone is ~30 km [18].

The mixing of fresh and saline waters at a tidal river mouth depends on the volumetric proportions of river water W entering the estuary within a tidal cycle and the tidal prism P. According to present-day data [10], the area of Mezen estuary is $F = 177$ km^2. The value of Simmons test $\alpha = W/P$ with the use of the values of Q and F, given above, yields $\alpha \sim 0.01$, i.e., the Mezen estuary is of the type of partially mixed estuaries with a weak stratification. Maximal salinity values in the mouth section $S \sim 21$–22‰ (late June) [16] were recorded in the period when the tidal flow changes from flood to ebb, and the minimal values of $S \sim 17$‰, at the inverse change of currents at the moment of zero flow velocity. A small temporary stratification of water forms because of velocity difference at different flow horizons.

Flow Velocity in the Estuary

At a large tide range (the mean values are 5.1 and 7.8 m for neap and spring tide, respectively), the flow has the same direction throughout Mezen EM: toward the estuary head during flood tide (inverse flow) and toward the sea during ebb tide (direct flow). The calculation of the mean phase velocity of tidal wave propagation from Semzha V. to the section at Belyi Nos Cape based on data in [2] yields $c = 6.9$ m/s. The tidal current in the Semzha V. section reaches its maximum velocity of 1.8 m/s 3 h after the low tide and 2–3 h before the flood tide. According to measurements [3], the velocity of tidal current was maximal ($\overline{U} \sim 3$ m/s) in the section at Tolstik C. (near Okulovsk), where a tidal bore described in [33] was observed.

METHODS OF STUDIES

Tidal wave propagation into a funnel-shaped estuary is the focus of many studies [7, 11, 17, 29, 30, 35]. Tidal wave transformation during its propagation into an estuary depends on the decrease rate of estuary cross-section area in the direction from the mouth section toward its head. In mathematical descriptions of wave motion in an estuary the narrowing of the river mouth in the horizontal (river width B) and vertical plane (river depth H) is approximated by exponential functions of the form:

$$B = B_0 e^{-x\beta}, \quad H = H_0 e^{-x\gamma}, \tag{1}$$

where x is the distance along the estuary, $x = 0$ is EM; B_0 and H_0 are flow width and depth at $x = 0$; $\beta = 1/l_b$ and $\gamma = 1/l_h$ are the coefficients of channel narrowing

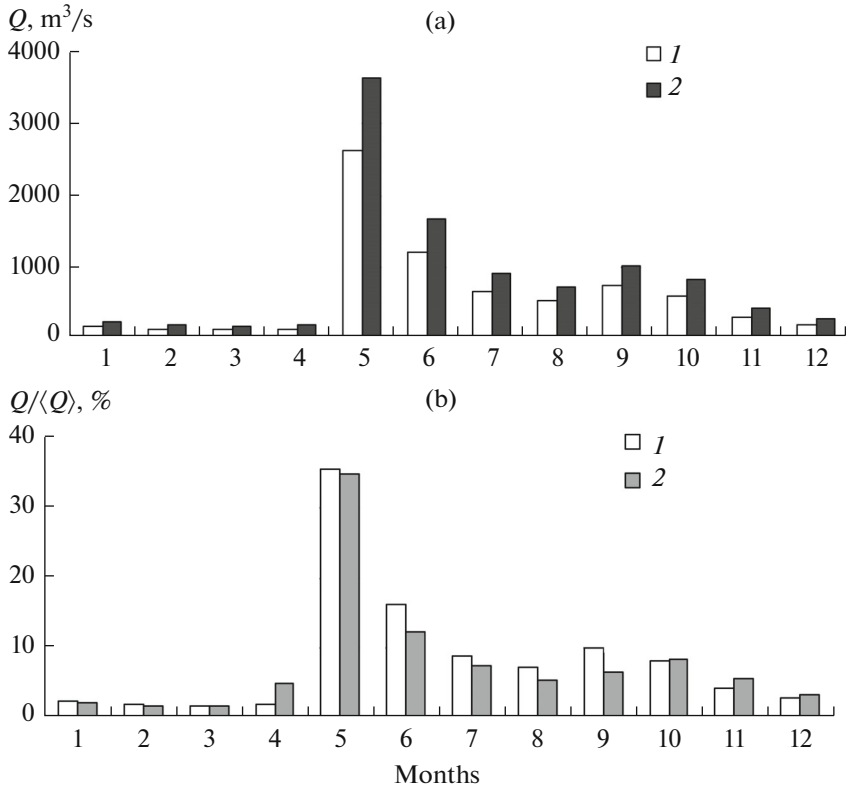

Fig. 4. Annual variations of mean monthly water discharges over period 1985–1987: (a) (*1*) at Malonisogorskaya g. s., by data in [1], and (*2*) at Mezen mouth, by the author's estimate; (b) (*1*) annual runoff distribution, %, at Malonisogorskaya g. s. over 1985–1987, by data in [1], and (*2*) at Mezen g. s. (EH) over 1920–1976, by data in [17].

because of a decrease in its width and depth with dimension of 1/km, the values of l_b and l_h determine the distances from EM at which the changes in estuary width and depth follow an exponential law.

The coefficients β and γ in (1) show the rate of changes in the channel cross-section area. At a distance l_b from EM (1) the channel width decreases by 35%, and this characteristic can be calculated by maps (Google Earth) [34].

The tidal range in an estuary is governed by four major factors: (1) the inertia in the acceleration and deceleration of moving water mass; (2) bed hydraulic friction; (3) the decrease in estuary width B and depth H upstream the channel; (4) the partial reflection of the tidal wave from the steadily narrowing banks. As the first approximation, the propagation of a tidal wave into a narrowing estuary can be described by a system of one-dimensional linear equations of motion for shallow water. As $\beta \gg \gamma$ for many estuaries, the estuary bed is assumed horizontal. Despite the considerable idealization, such simplified model gives a good description of the amplitude M_2 of the tidal wave in the microtidal estuary of the Delaware R. [30]. Calculations by this analytical model, assuming linear friction and estuary width exponentially decreasing along it, show friction to reduce the amplitude and wavelength of the first harmonic of semidiurnal tide and to slow down its propagation into the estuary without changes in wave shape. In this case, the high-frequency components of the tidal wave show a faster decrease in wave amplitude, while in its low-frequency components the decrease in wave propagation velocity is faster. Conversely, the narrowing of the channel increases the amplitude and propagation velocity of the wave and decreases its length. The propagation velocity of the tidal wave in a narrowing estuary decreases because of wave polarization, which changes the character of water particle orbits in the tidal current, and the direction of flow concentrates along the dynamic axis of the channel [17, 29].

The propagation of tidal waves into a narrowing estuary is accompanied by changes in their shape, length λ, height, and motion velocity c. To take into account the nonlinear effects in the propagation of tidal wave in shallow water and to describe the transformation of its shape, balance equations of water energy in the estuary are used reflecting the decrease in B and H and involving a quadratic friction law, taking into account the hydraulic friction coefficient f [35]. An analytical solution yields the following expression for variation of tidal range h upstream the estuary:

$$\frac{dh}{dx} = 0.5(\beta + \gamma)h - \frac{f(\overline{U})^2}{3\pi g H \cos\varphi}, \quad (2)$$

where $\overline{U}$ is the maximal tidal flow velocity in the estuary, $f = 8g/C^2$ is hydraulic friction coefficient (C is Chezy coefficient), φ is the phase difference between the horizontal and vertical velocity components of tidal wave propagation.

Commonly, l_b in estuaries varies within 10–50 km, while the depth changes slower than the width and $l_b \ll l_h$. Now, considering that $\beta \gg \gamma$, we can neglect γ [35], to simplify (2):

$$\frac{dh}{dx} = 0.5\beta h - \frac{fh^2c^2\cos\varphi}{12\pi g(H_0)^3}. \quad (3)$$

The bed friction factor f in (2) is difficult to specify for a macrotidal estuary. If we neglect friction and denote the tidal range in the mouth section by h_0, equation (2) will give a simple expression $h/h_0 = e^{0.5(\beta+\gamma)x}$, i.e., the tidal range grows exponentially at an exponential decrease in estuary width and depth.

Depending on the change in tidal wave amplitude along the narrowing estuary, all estuaries are divided into 3 types: a wide and deep estuary ($\beta \sim 2k$, k is the wave number of the tidal wave), in which the contributions of estuary narrowing and friction to the effect on the wave are in equilibrium, such that the wave moves without transformation at some distance from EM; a long estuary ($\beta > 2k$; the effect of narrowing dominates over that of friction, and wave amplitude increases with the distance from EM); a short estuary ($\beta < 2k$; the effect of friction is greater than that of the narrowing estuary, and the wave amplitude decreases with the distance from EM) [31, 35]. The estimates given above were obtained in [35] analytically under the assumption that $\beta \gg \gamma$, i.e., the estuary bed is horizontal.

In macrotidal, shallow, and funneled estuaries with low river runoff, an inverse tidal wave (tidal bore), undular or collapsing, may form. The collapsing tidal bore forms during spring tide at largest change in water level. As the tidal wave moves upstream a river in narrow and shallow segments of river mouth, the wave front becomes steeper, resulting in a collapse. In wider and deeper parts of the channel, the tidal bore may disappear to form again in narrow channel segments further upstream. The mathematical apparatus [22, 24], developed to study the motion of a undular and collapsing tidal bore along an estuary, can be used to describe the oscillations of the free surface of a undular tidal bore with the use of the known equations of wave transformation on shallow water, whose solution yields a sinusoidal shape of tidal bore surface. The solution of Korteweg–de Vries equation in the form of a cnoidal wave function can be used to describe an undular tidal bore in a river in more detail [22]. The data of measurements and simulation are in good agreement, although neither linear wave theory nor the cnoidal wave function describe the asymmetric shape of tidal bore wave and details of the profile of free water surface [5].

In the analysis of the landward motion of an inverse wave in an estuary, the possible formation of a tidal bore in an individual estuary is assessed with the use of Fr_b number in the following form [22]:

$$\mathrm{Fr}_b = \frac{U + V}{\sqrt{gH}}, \quad (4)$$

where V is cross-section-averaged flow velocity positive downstream toward river mouth; U is the velocity of wave motion toward estuary head; g is free fall acceleration; H is river depth before tidal-bore arrival.

For a tidal bore to form in an estuary, the condition $\mathrm{Fr}_b > 1$ is to hold [21, 22, 30]. The first tidal bore wave is commonly accompanied by a series of well-developed wave formations with smaller amplitude; in this case, the start of first wave collapse is determined by criterial Fr_b, whose values vary within wide limits. Experiments in a laboratory flume showed no transformation of an undular tidal bore into a collapsing bore at $\mathrm{Fr}_b \le 1.4$ [28], while, as reported in [5, 22], the collapse takes place only at $\mathrm{Fr}_b > 1.5$–1.8. The range of Fr_b variations as wide as that is due to an ambiguity in evaluating the variables in (4), especially, in the case of natural tidal bores. To evaluate the Froude number by (4) requires measured values of flow velocity and mean flow depth. The active motion of sediments and variations in bed relief at the propagation of a tidal bore wave into an estuary cause ambiguity in the evaluation of variables in (4), in particular, the mean flow depth [32]. The author generalized and analyzed measurement data to improve the formula for assessing Fr_b, which includes H, averaged over the given cross-section:

$$\mathrm{Fr}_b = \frac{U + V}{\sqrt{g\dfrac{A}{B}}}, \quad (4a)$$

where A, B are the cross-section area and the width of the channel before tidal bore arrival; $H = A/B$.

The expression (4a) can be used to evaluate Fr_b for the section under consideration and to find whether a tidal bore can form in the given section of the estuary.

TIDAL WAVE TRANSFORMATION AND TIDAL BORE FORMATION IN THE MEZEN ESTUARY

The Effect of Mouth Shape on Tidal Height

As mentioned above, some transformation of the tidal wave starts as early as the Mezen Gulf. At the propagation of the wave from the gulf into the narrowing estuary through the reach Maslyanyi Cape–

Table 1. Variations of h, the time of water level rise t_1 and drop t_2 at gauging stations along Mezen estuary 3 days before a neap tide in July 2007 (top number) [3], during spring tide in the summer of 1968 [13] (bottom number); Fr_b numbers in estuary cross-sections, calculated for the conditions of flood (top number) and ebb (bottom number) tide (the dash means no measurement data available)

Gauges	x, km	h, m	t_1, h	t_2, h	t_1/t_2	Fr_b
Ryabinov Cape	0	– 7.6	– 4.83	– 7.58	– 0.63	TC 0.23 LT 0.7
Semzha V.	6	5.8 7.82	6.00 4.65	6.50 7.9	0.92 0.59	TC 0.61 LT 1.1
Vasil'evich Cape	9	5.1 7.46	5.00 4.0	7.50 8.1	0.67 0.49	TC 0.91 LT 1.1
Tolstic Cape	15	–	–	–	–	TC 0.78 LT 1.0
Okulovsk V.	17	4.2 5.84	4.75 3.35	7.75 8.9	0.68 0.38	TC 1.07 LT 1.8
Chetsa V.	22	–	–	–	–	TC 0.52 LT 1.0
Morozilka V.	27	3.1 4.44	4.25 2.78	8.00 9.87	0.53 0.28	TC 0.4 LT 0.9
Kamenka Setll.	36	2.7 3.74	3.50 2.5	9.00 10.00	0.39 0.25	TC 0.71(1.1) LT 1.3
Belyi Nos Settl.	39	2.3 3.28	4.50 2.42	8.25 10.00	0.55 0.24	TC 0.7 LT 1.5

Semzha V., the tidal range slightly increases (Table 1). The amplitude of level variations decreases further along the entire estuary from Semzha g. s. to EM, i.e., bed friction at all segments of the estuary is large and the second term in (2) exceeds the first term. The predominant role of friction in tidal wave transformation is confirmed by the comparison of variations of h/h_0 along the Mezen estuary, calculated by (2) with bed friction neglected, with data of measurements in different estuary sections during neap tide [2, 3]. Figure 5 also gives data of measurements of the relative tidal range during spring tide [13]. Measured values of the relative tidal range during spring tide are also given for comparison [13]. Note that the measured values of the relative tidal range during spring and neap tide in 2007 and 1968 are the same. An exponential approximation of these data yields $h/h_0 = \exp(-0.025x)$, the coefficient at x is a constant characterizing the estuary; in the case of the Mezen estuary, this coefficient is 40 km, i.e., the estuary length.

The nonlinear dependence of tidal wave shape on the bed hydraulic friction in shallow areas contributes to an increase in the propagation velocity of wave crest and to a decrease in the velocity of wave trough, resulting in wave distortion, i.e., a decrease in the duration t_1 of the rise and an increase in the duration t_2 of the drop of the tide level. The decrease in t_1/t_2 is due to energy transfer from tidal component M_2 to M_4 and an increase in the amplitude ratio M_4/M_2, which becomes especially vivid at a distance of 27 km from EM (Table 1; Fig. 6). The active energy transfer from the first harmonic M_2 to the following harmonics generally causes a decrease in the rate of tidal level rise [4, 30]. The water levels, given in Table 1 and Fig. 6, were measured in 2007 3 days before the neap tide (h = 4.5 m, Semzha g. s.) [3]. The comparison of these data with the values of t_1/t_2, measured during the spring tide of 1968 [13] and given in Table 1, shows a regular decrease in ratio t_1/t_2 during spring tide faster than that at lower tide. The same will be the effect of an increase in Q during summer freshets at about the same h at estuary mouth [5, 30].

Let us assess the effect of Mezen estuary shape with the parameters of narrowing β and γ in (1) on tidal range and tidal wave parameters during its propagation into the estuary. Estuary width in the mouth section is 9.0 km. Further upstream, estuary width gradually decreases to reach 1.2 km at estuary head. The rate of estuary narrowing was evaluated by (1) with flow characteristics in the Mezen estuary provided by N.A. Demidenko (State Oceanographic Institute). The calculation of narrowing parameters typical of the Mezen estuary at neap tide crest (TC) yields the values of B_0 = 9.3 km and H_0 = 9.3 m, while the distances l_b and l_h are 18.6 and 45 km, respectively ($\beta = 0.0538$, $\gamma = 0.0221$ 1/km (Table 2)). The depths used in the calcu-

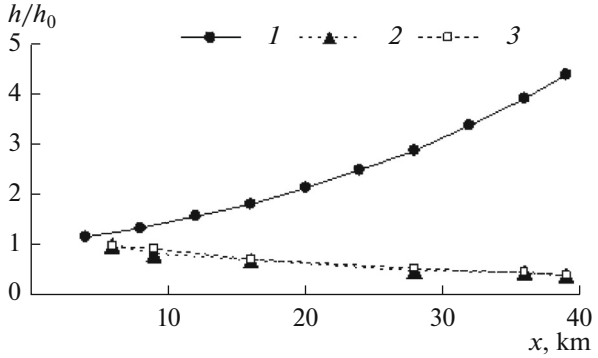

Fig. 5. Variation of the relative tide height along Mezen R. estuary: (*1*) calculation by (3) with bed friction not taken into account at $\gamma = 0.0221$ 1/km; (*2*) calculation by water levels measured at estuary g. s. [3] 3 days before the neap tide; (*3*) calculation of h/h_0 by data of tide height measurements during spring tide [13].

lations were averages over appropriate cross-sections, and the obtained value $H_0 = 9.8$ m can be used to evaluate Fr_b by (4a). The value of H_0 differs from the depth $\langle H \rangle$, averaged over the length of the estuary at TC, as $\langle H \rangle = 7.4$ m. The calculation of estuary narrowing parameters at low tide (LT) yields $B_0 = 3.0$ km and $H_0 = 1.8$ m, $l_b = 17.5$, $l_h = 64$ km ($\beta = 0.057$, $\gamma = 0.016$ 1/km), and $\langle H \rangle = 1.7$ m. Thus, the coefficients β and γ estimated for TC conditions differ ~2.5 times, and those for LT, ~3.5 times. In both cases, we cannot neglect γ compared to β, as it is often possible in many other estuaries [35].

The comparison of parameter β with the wave number for tidal wave allows us to determine whether the wave amplitude will increase or decrease during its motion along the estuary. The calculation for TC with $\langle H \rangle$ taken into account yields $\beta > 2k$ (Table 2), i.e., wave amplitude will increase toward estuary head. This estimate contradicts the results of measurement (Fig. 5). The calculation at LT yields a plausible result: $\beta < 2k$, i.e., a decrease in tidal wave amplitude during the motion toward EH. The estimate $\beta > 2k$, obtained at flood tide shows that, in a shallow estuary with a considerable bed slope, variations in the depth cannot be neglected in the analysis of tidal wave evolution along the estuary.

Criterion of Bore Formation—Froude Number

In the river reach between Tolstik Cape and Okulovsk V., where the tidal bore described in [33] took place in the XIX century, four branches form under current conditions at low tide, two of which are 0.5 m in depth, another branch is 1.7 and the last is 0.8 m in depth. The estimation of Fr_b for this section shows that the bore can form in one of shallow branches (Table 1).

As mentioned above, in the reach from Okulovsk to estuary head (Mezen g. s.), a series of islands forms along the right bank, separating two longitudinal parts of river channel. In the section at Kamenka V., Vanina Koshka Isl. divides the channel into two branches, where, at minimal water level $\mathrm{Fr}_b < 1$ for the entire section (Table 1). However, calculations by (4a) for the shallow right-hand branch, where a tidal bore took place (Fig. 1), yields $\mathrm{Fr}_b = 1.3$, at which a collapsing tidal bore can form [28]. The mobility of estuary bed and the passage from Morozilka section with a depth 3 times that in the Kamenka section facilitate the formation of a collapsing crest of the first tidal bore wave. The values of Fr_b, given in Table 1 for low tide are ~1.0 in many sections, implying the possible formation of an undular tidal bore. For the Mezen estuary at average values of c and H (during low tide), $\mathrm{Fr}_b = 1.7$, suggesting the possible formation of a collapsing bore in Mezen estuary.

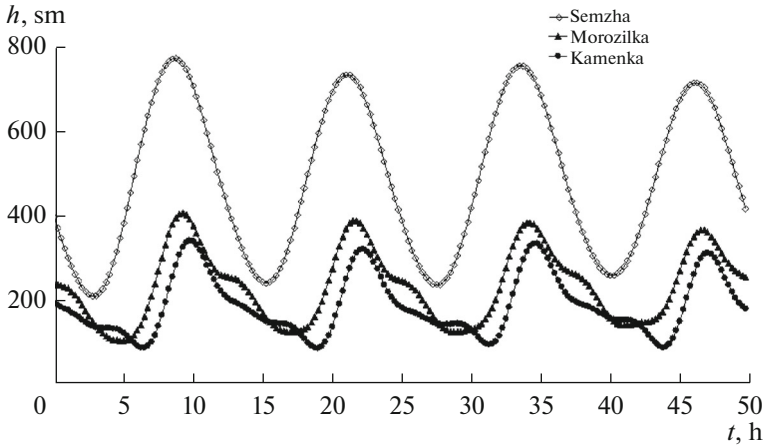

Fig. 6. Water level variation in Mezen estuary at Semzha g. s. (6 km from EM), Morozilka g. s. (27 km), and Kamenka g. s. (36 km) by data in [3].

Table 2. Characteristics of river mouths and semidiurnal tide waves, propagating in the estuary: mean estuary depth H, parameters β and γ were calculated for tide crest and low tide when data are available ("+" means there is a tidal bore in the estuary, and "–" means no bore)

Estuary, L, km	Q, m^3/s	H, m	β	γ	h, m	k, rad/km	β, $2k$	Tidal bore
Mezen, 40	780	TC – 7.4	0.0538	0.022	7.8	0.017	$\beta > 2k_0$	+
		LT – 1.7	0.057	0.015		0.032	$\beta < 2k$	
Qiantang*, 122	1000	TC – 7.0	0.0263	0.013	8.9	0.017	$\beta < 2k$	+
		LT – 2.3	–	0.018		0.03		
Seine*, 50	430	8	0.0318	–	7.5	0.016	$\beta \sim 2k$	+
Garonne*, 64	600	5	0.0381	–	6.0	0.02	$\beta < 2k$	+
St. Lawrence, 600	12000	350	0.0073	0.0049	2.3	0.0024	$\beta > 2k$	–
Delaware*, 218	335	30	0.032	0.0023	1.2	0.008	$\beta > 2k$	–

* The estuaries were described in detail in [4].

PROPAGATION OF TIDAL WAVES IN DIFFERENT ESTUARIES

To analyze the evolution of tidal wave at river mouths, several estuaries were chosen with characteristics given in Table 2. The amplitude of a tidal wave entering an estuary is known to show the effect of a decrease in estuary cross-section area from EM to EH and the hydraulic friction at the bed and banks. In addition, the thickness of the Stokes layer $d = \sqrt{AT}$ (A is turbulent exchange coefficient, T is wave period), which forms near flow free surface, plays a significant role in wave transformation in an estuary [8]. At the propagation of a semidiurnal wave in a shallow estuary, in which a tidal bore forms, A varies within the range of 0.02–0.1 m^2/s [5, 8], when the thickness d varies within 30–67 m and flow regime in the estuaries under consideration, except for that of St. Lawrence R., can be considered gradient-viscous. Estimating the effect of estuary shape on tidal wave amplitude during its propagation into the estuary yields interesting results (Table 2).

The comparison of parameter β with the wave number of tidal wave in different estuaries shows that in relatively deep micro- and meso-tidal estuaries, wave transformation is taking place with an increase in its amplitude toward estuary head, as, for example, in the estuaries of St. Lawrence and Delaware. This estimate is supported by the data of studies given in [4, 6]. In the microtidal estuary of the Delaware R., we have $H \sim d$, and wave amplitude first decreases at the entry into the estuary and next increases to become at EH twice as large as that at EM, notwithstanding the small h in EM. The change in wave amplitude along estuary such as that in the Delaware in most cases can be adequately described analytically for estuaries with $H \sim d$ [8]. A small waterfall upstream of EH (Trenton T.) prevents the tidal level variations from propagation upstream, and the friction forces have not enough time to cause changes in wave amplitude [4]. In the estuary head of the St. Lawrence R., the spring tidal range is twice that in EM, and the tidal level variations disappear at a distance of ~100 km further upstream. The narrowing of channels in such estuaries follows the law (1) with the widths of Delaware and St. Lawrence estuaries decreasing 1.7 and 7.4 times slower than that of the Mezen, respectively. In both estuaries, the estimate $\beta > 2k$, with depth variations neglected, yields an increase in wave amplitude toward EH, which is confirmed by observations.

The depths of macrotidal estuaries, whose characteristics are given in Table 2, are much less than Stokes layer, and the amplitude of tidal waves should decrease under the effect of turbulent friction. This is the case in the estuaries of the Mezen at LT and the Qiantang at TC. Note that estimating the parameter of estuary narrowing of the Qiantang R. before channel improvement operations in the estuary yields $\beta = 0.0244$, i.e., according to the estimate $\beta < 2k$, tidal wave amplitude also decreases toward EH. Considering that the values of β before and after Qiantang estuary improvement are of the same order and that those values for TC and LT in the Mezen differ only in the third digit after the decimal point, we can suppose that the inequality $\beta < 2k$ also holds for LT in the Qiantang estuary. According to data in [25], tidal range decreases on the average by half from EM to EH. The estimation of l_b after channel improvement yields $l_b = 38$ km; this is the distance from EM (Ganpu T.) at which a 50-km-long segment begins where several tidal bores form. The estimate $\beta > 2k$, obtained for the Mezen at TC with depth variations along the estuary not taken into account yields a result in contradiction with data, i.e., an increase in wave amplitude toward EH. The longitudinal profile of Mezen estuary bed abruptly changes; therefore, γ is to be taken into account in describing tidal range variations along the estuary.

In the Garonne estuary, $\beta \sim 2k$, implying that, within some segment of the reservoir, the wave propagates without significant changes in its shape. Studies of tidal waves in Garonne estuary confirm this conclusion. According to data in [20], tidal range in the estu-

ary does not change (~6 m) at a distance of 30 km from EM; it decreases 1.5 times in the following 15 km to reach 0.2 m at a distance of 64 km from the mouth. For the Seine R. estuary, before its embankment, $\beta \sim 0.1$ 1/km [20, 34], which is greater than the values obtained for other estuaries. In this case, according to estimate $\beta > 2k$, the amplitude of the tidal wave is to increase toward EH. The estimate of β given in Table 2, which has been calculated for the channel after improvement, suggests a decrease in wave amplitude during the propagation in the estuary, which is in agreement with observational data: the tidal range in the Seine estuary decreases toward EH during spring tide or keeps unchanged during neap tide [36].

Tidal Bore Formation

Thus, in deep estuaries with $H \geq d$, the tide amplitude increases during wave propagation along the estuary; however, no tidal bore forms in this case (Table 2). In shallow estuaries with $H < d$, the amplitude of the tidal wave decreases at its propagation from the mouth toward estuary head. In some segments of such estuaries, a tidal bore can form at an abrupt decrease in the depth. After its formation, the depth at the front section abruptly increases and water flow can be described with the use of the law of moving hydraulic jump. In the analysis of the conditions of tidal bore formation and disappearance, of interest are the macrotidal estuaries of the Seine [34] and Qiantang [25] rivers, where artificial deepening of tidal channel leads to a rapid change in the shape characteristics of estuary cross-section. Table 2 gives the characteristics of these estuaries after channel improvement. In the XIX century, one of the highest tidal bores was recorded in the Seine estuary. It showed a crest height of up to 7.5 m and a propagation velocity of up to 10 m/s [5]. The tidal bore propagated over 80 km from EM. After the start of channel improvement, the tidal bore disappeared; however, later it appeared again because of the gradual decrease in the depth caused by sediment inflow into the channel. The embanking and regular dredging operations to ensure stable navigation depth ($H = 6$ m) in Seine estuary caused the disappearance of this huge tidal bore and the formation of an indistinguishable undular tidal bore with small wave steepness 45 km upstream of its original location [21]. The low-frequency undular tidal bore, first identified during the spring tide in the autumn dry season of 2011, shows $\mathrm{Fr}_b = 1.07$ and a height of the first wave of 1.02 m. Thus, the deepening of the estuary changed the character and localization of the tidal bore at the Seine mouth.

Global channel-improvement operations aimed to reduce tide inundation area were carried out in Qiantang estuary in the 1960–1990s [5, 25]. Despite the large area becoming available for industry and agriculture (730 km^2) and the change of estuary hydrological regime, the value of channel narrowing parameter has the same order as it had before the embankment. As the tidal bore that forms at Qiantang mouth is the highest in the world, attracting many tourists visiting the site, it was desirable to preserve the tidal bore during channel improvement operations. It still forms in several sections in the reach 38–88 km from EM. The beginning of this reach is determined by parameter l_b from (1). Before channel embankment, $\mathrm{Fr}_b = 2.5$ [5], and after it, $\mathrm{Fr}_b = 2.1$.

The Garonne estuary has segments with the formation of several branches, separated by islands, making this estuary morphologically similar to that of the Mezen. Studying the propagation of the tidal wave into the Garonne estuary during low-water seasons showed that, in some cases at small H and Q, the tidal bore can form even during a neap tide ($\mathrm{Fr}_b \sim 1.1$) [20]. In the range $1 < \mathrm{Fr}_b < 1.1$, a low-frequency tidal bore with a high wavelength-to-depth ratio of 20–40 was recorded in the Garonne estuary. In a narrow branch of the Garonne estuary at small depth and $\mathrm{Fr}_b \sim 1.1$, a collapsing reverse wave was recorded, which was referred to as a collapsing atypical tidal bore in [19]. A similar tidal bore, which forms at Kamenka section in the Mezen estuary, is described above.

The analysis of the formation conditions of the tidal bore shows a strong effect of the depth on tidal wave height during its propagation into the estuary. The parameter γ, which characterizes depth variations, in the case of shallow estuaries is of the same order as β and an order of magnitude greater than γ for deep estuaries. In the analysis of tidal wave transformation in shallow estuaries, the relationship $\beta \gg \gamma$ is not valid, and depth variations are to be taken into account.

CONCLUSIONS

The mean annual water discharges at the Mezen mouth during summer low-water season were estimated at 888 and 713 m^3/s in July and August, respectively. In this period, the formation of a tidal bore is most likely. The parameters characterizing estuary narrowing in the planar view and over depth during flood and ebb tide were determined, and their contribution to changes in the amplitude of tidal wave along the estuary was evaluated. The effect of friction dominates in the transformation of the tidal wave in the reach from Semzha V. to Mezen T., and wave amplitude decreases in the course of its propagation into the estuary. The comparison of the parameter of channel narrowing in the planar view with the wave number of tidal wave showed that variation of the longitudinal profile of estuary bed is to be taken into account to obtain a reliable estimate of tidal wave transformation in a shallow macrotidal estuary. The values of Fr_b were calculated for several channel cross-sections at high and low tide. In a half of cross sections at low tide, we have $\mathrm{Fr}_b > 1$, suggesting the possible formation of a

tidal bore, especially in narrow and shallow erosion channels into which the channel divided.

The analysis of variations of channel narrowing parameters for different estuaries showed that, in relatively deep micro- and mesotidal estuaries, the amplitude of tidal wave increases toward EH, as can be evaluated by the relationship $\beta > 2k$. Estimates $\beta < 2k$ and $\beta \sim 2k$ were obtained in most cases for shallow macrotidal estuaries, showing that the effect of friction force on the tidal wave amplitude dominates over the effect of channel shape or such effects are equal. The problem of tidal wave evolution in shallow estuaries should be formulated taking into account channel narrowing resulting from depth variations, because $\beta \sim \gamma$.

Regular channel-deepening operations in the estuary at the Seine mouth result in the disappearance of a tidal bore with a high collapsing crest and in the formation of a low-frequency undular tidal bore with small wave steepness further upstream. The comparison of Mezen and Garonne estuary channels showed that a collapsing tidal bore can form at a relatively low Fr_b (1.1) in narrow shallow branches.

The features that play a significant role in the formation of a tidal bore in an estuary include the shape of channel cross-section, the separation of the channel into several branches, and the large variability of longitudinal profile of the bed in a macrotidal estuary.

ACKNOWLEDGMENTS

The author is grateful to N.A. Demidenko (State Oceanographic Institute) for provided data of expedition studies in Mezen estuary.

This study was supported by the Russian Foundation for Basic Research, project nos. 16-05-00288 and 16-05-00209.

REFERENCES

1. *Gosudarstvennyi vodnyi kadastr. Mnogoletnie dannye o rezhime i resursakh poverkhnostnykh vod sushi* (State Water Cadaster. Long-Term Data on the Regime and Resources of Surface Continental Waters), P. 1, vol. 1, no. 8, 1986–1988.
2. Demidenko, N.A., Hydrological regime of Mezen Gulf and the estuaries of the Mezen and Kuloi, in *Sistema Belogo moray*, (White Sea System), vol. II, Moscow: Nauch. mir, 2012, pp. 411–32.
3. Demidenko, N.A., Efimova, L.E., Efremova, N.A., and Yurkin, M.M., Hydrometeorological regime of Mezen and Kuloi estuaries and possible changes at the construction of the Mezen TPP, in *"Ekologiya arkticheskikh i priarkticheskikh territorii." Tr. Mezhdunar. Simpoz.* (Ecology of Arctic and Near-Arctic Territories, Proc. Intern. Symp.), Arkhangel'sk, 2010, pp. 70–72.
4. Dolgopolova, E.N., Sediment transport and saltwater intrusion into the weakly stratified estuary of the Delaware R., *Water Resour.,* 2014, vol. 41, no. 2, pp. 143–162.
5. Dolgopolova, E.N., The conditions for tidal bore formation and its effect on the transport of saline water at river mouths, *Water Resour.*, 2013, vol. 40, no. 1, pp. 16–30.
6. Dolgopolova, E.N. and Isupova, M.V., Water and sediment dynamics at Saint Lawrence River mouth, *Water Resour.*, 2011, vol. 38, no. 4, pp. 453–469.
7. Zyryanov, V.N., Nonlinear pumping-effect in oscillation processes in geophysics, *Water Resour.*, 2013, vol. 40, no. 3, pp. 243–253.
8. Zyryanov, V.N. and Chebanova, M.K., Tidal waves in an estuary, *Prots. Geosred.*, 2015, vol. 3, no. 3, pp. 21–33.
9. *Kachestvo morskikh vod po gidrokhimicheskim pokazatelyam. Ezhegodnik 2012* (Seawater Quality by Hydrochemical Characteristics: Yearbook 2012), Korshenko, A.N, Ed., Moscow: Nauka, 2013.
10. Kravtsova, V.I. and Mit'kinykh, N.S., *Ust'ya rek Rossii. Atlas kosmicheskikh snimkov* (River Mouths in Russia. Atlas of Space Photographs), Mikhailov, V.N., Ed., Moscow: Nauch. mir, 2013.
11. Lapina, L.E., *Dinamika techenii i osobennosti perenosa konservativnoi primesi v ust'evykh oblastyakh prilivnykh rek* (Dynamics of Flows and Specific Features of a Nonreactive Solute Transport in Mouth Areas of Tidal Rivers), Syktyvkar: Inst. Matem. Mekh., Ural.Otd., Russ. Akad. Sci., 2001.
12. White Sea Pilot Chart, http://rivermaps.ru/doc/beloe/beloe-3.htm.
13. Mikhailov, V.N., *Ust'ya rek Rossii i sopredel'nykh stran: proshloe, nastoyashchee i budushchee* (River Mouths of Russian and Nearby Countries: Past, Present, and Future), Moscow: GEOS, 1997.
14. Mikhailov, V.N. and Gorin, S.L., New definitions, regionalization, and typification of river mouth areas and estuaries as their parts, *Water Resour.,* 2012, vol. 39, no. 3, pp. 247–260.
15. Mishin, D.V., Mezen', in *Reki i ozera mira. Entsiklopediya* (World Rivers and Lakes. Encyclopedia), Moscow: Entsiklopediya, 2012, pp. 414–416.
16. Mishin, D.V., Assessing the variability of hydrological characteristics in Mezen estuary during a tidal cycle, *Sb. Tr. VII-i Vsesoyuz. Konf. "Dinamika i termika rek, vodokhranilishch i pribrezhnoi zony morei"* (Coll. Pap. VII All-Union Conf. "Dynamics and Thermal Regime of Rivers, Reservoirs, and the Coastal Zone of Seas"), Moscow, 2009, pp. 463–470.
17. Polonskii, V.F., Lupachev, Yu.V., and Skriptunov, N.A., *Gidrologo-morfologicheskie protsessy v ust'yakh rek i metody ikh rascheta* (Hydrological–Morphological Processes at River Mouths and Methods of Their Calculation), St. Petersburg: Gidrometeoizdat, 1992.
18. *Estuarno-del'tovye sistemy Rossii i Kitaya: gidrologo-morfologicheskie protsessy, geomorfologiya i prognoz razvitiya* (Estuarine–Deltaic Systems of Russia and China: Hydrological-Morphological Processes, Geomorphology, and Development Forecasts), Korotaev, V.N, Mikhailov, V.N, Babich, D.B, and Shuguan, L., Eds., Moscow: GEOS, 2007.
19. Bonneton, P., Parisot, J.-P., Bonneton, N., et al., Large amplitude undular tidal bore propagation in the Garonne River, France, *Proc. of 21-st Int. Offshore and*

Polar Eng. Conf., Maui, Hawaii, 2011, V. III, pp. 870–875.

20. Bonneton, P., Van de Look, J., Parisot, J-P., et al., On the occurrence of tidal bores – the Garonne River case, *J. of Coastal Res., Special Issue 64, Proc. 11th Int. Coastal Sympos.,* 2011, pp. 1–4.
21. Bonneton, N., Bonneton, P., Parisot, J-P., et al., Tidal bore and Mascaret – example of Garonne and Seine Rivers, *Publie´par Elsevier Masson SAS pour l'Acade´mie des sciences,* 2012. http://dx.doi.org/10.1016/j.crte.2012.09.003
22. Chanson, H., Environmental, ecological and cultural impacts of tidal bores benaks, bonos and burros, *Proc. IWEH. Int. Workshop on Environ. Hydraulics: Theoretical, Experimental and Computational solutions,* Valencia, 2009, pp. 1–20.
23. Dolgopolova, E.N. and Mishin, D.V., Conditions of tidal bore formation in the Mezen estuary, *Proc. of Tidal Bore Workshop: Recent Study and Future Researches,* Caen, France, 2015, p. 11.
24. Donnelly, C. and Chanson, H., Environmental impact of undular tidal bores in tropical rivers, *J. Environ. Fluid Mechanics,* 2005, vol. 5, no. 5, pp. 481–494.
25. Han, Z., Xuy, Z., Lin, B., and Xuan, W., Variation of tides and river regime after river training in the Qiantang estuary, *Proc. Int. Conf. Estuaries and Coasts, Hangzhou, China*, 2003, pp. 66–80.
26. http://vsereki.ru/severnyj-ledovityj-okean/bassejn-belogo-morya/mezen.
27. http://vk.com/video65200071_167250426.
28. Koch, C. and Chanson, H., Turbulence measurements in positive surges and bores, *J. Hydrol. Res.,* 2009, vol. 47, no. 1, pp. 29–40.
29. Lynch, D.K., Tidal bores, *Scienific American,* 1982, vol. 247, no. 4, pp. 134–143.
30. Parker, B.B., *Tidal hydrodynamics,* New York: Wiley, 1991.
31. Prandle, D., *Estuaries,* Cambridge: Cambridge Univ. Press, 2009.
32. Reungoat, D., Chanson, H., and Caplan, B., *Field measurements in the tidal bore of the Garonne River at Arcins (June 2012),* 2012, Brisbane: Univ. Queensland, St Lucia QLD, Australia.
33. Reineke, M., *Description hydrographique des COTES SEPTENTRIONALES DE LA RUSSE. Premiere Partie. MER BLANCHE*, Paris: Imprimerie Administrative de Paul Dupont, 1860.
34. Tessier, B., et al., Infilling stratigraphy of macrotidal tide-dominated estuaries. Controlling mechanisms: sea-level fluctuations, bedrock morphology, sediment supply and climate changes (The examples of the Seine estuary and the Mont-Saint-Michel Bay, English Channel, NW France), *Sedim. Geol.,* 2012, vol. 279, pp. 62–73.
35. Van Rijn, L.C., Analytical and numerical analysis of tides and salinity in estuaries. Pt. I, *Ocean Dynamics,* 2011, vol. 61, pp. 1719–1741.
36. Verney, R., Brun-Cottan, J-C., Lafite, R., Deloffre, J., and Taylor, J.A., Tidally-induced shear stress variability above intertidal mudflats. Case of the macrotidal Seine estuary, *Estuaries and Coasts,* 2006, vol. 29, no. 4, pp. 653–664.

Translated by G. Krichevets